Engineering Structures 222 (2020) 111090

Contents lists available at ScienceDirect

Engineering Structures

journal homepage: www.elsevier.com/locate/engstruct

Probabilistic calibration of fatigue safety factors for offshore wind turbine concrete structures

Joey Velarde[a,b,*], Amol Mankar[b], Claus Kramhøft[a], John Dalsgaard Sørensen[b]

[a] Marine and Foundation Engineering, COWI A/S, 8000 Aarhus, Denmark
[b] Department of the Built Environment, Aalborg University, 9220 Aalborg, Denmark

ARTICLE INFO

Keywords:
Offshore wind turbines
Fatigue reliability
Concrete structures
Code calibration
Probabilistic design
Gravity-based foundations

ABSTRACT

Current fatigue design rules for offshore concrete structures were adopted from the oil and gas industry. When better models or more information are available, partial safety factors can be re-calibrated according to target reliability levels for offshore wind turbines. This paper describes a framework for reliability-based calibration of fatigue partial safety factors for offshore wind turbine concrete structures. Offshore wind turbine loads accounting for the statistical distribution of turbulence intensity are estimated using a fully-integrated aeroelastic model. Based on available experimental fatigue tests, a fatigue reliability model for concrete is formulated and applied in two numerical examples. Results indicate that the recommended material partial safety factor in the DNV standard for *Offshore Concrete Structures* can be lowered without compromising structural safety. The proposed modification can potentially contribute to structural design optimization and further cost reduction in offshore wind energy.

1. Introduction

The offshore wind energy industry has significantly matured during the last two decades in terms of rated capacities of offshore wind turbines (OWTs), relative scale of support structures and depth of installations. Today, OWTs with rated capacities of 10 MW to 14 MW are typically supported by up to 9 m diameter monopiles and installed at wind farm sites with up to 40 m water depth. Alternative to monopiles, concrete gravity-based foundations (GBF) are attractive solutions particularly at shallow to moderate water depths or at site conditions where piling of monopiles exhibit geotechnical challenges. Currently, applications of the GBF were demonstrated for up to 5 MW capacity installed at shallow to moderate water depths in Denmark, Sweden and Belgium [1,2]. As wind turbine size increases and installations reach further offshore, concrete GBFs can potentially become more cost-effective solutions compared to traditional steel monopiles.

Continuous developments in the industry introduce uncertainties and changes in the loading environment, which make fatigue a more important issue in designing state-of-the-art support structures. Probabilistic methods can be applied to assess the structural reliability of OWT support structures. Most applications of reliability methods have been demonstrated in wind turbine blades [3–7] and wind turbine components [4,8]. Fatigue reliability analyses of support structures have also been demonstrated in several papers [9–13], mostly for assessment of wind turbine steel towers, monopiles and jacket foundations. Since current fatigue design rules for offshore concrete structures were adopted from the oil and gas industry, a re-assessment of these design rules for offshore wind turbines becomes important for structural design optimization.

This paper presents a re-assessment of fatigue safety factors for OWT concrete foundations by accounting for relevant load and resistance model uncertainties. Based on available experimental fatigue tests, a fatigue reliability model for concrete is formulated and applied in two numerical examples. The material partial safety factors are recommended based on target reliability levels for offshore wind turbines. Lastly, the sensitivity of concrete fatigue reliability to stochastic parameters are also presented.

2. Fatigue design factor calibration

In addition to selecting characteristic values, structural design codes and standards recommend partial safety factors to account for load and resistance model uncertainties. The consequence of failure is also accounted by these partial safety factors, which were traditionally selected based on sound judgement, accummulated experience or a combination of both. But during the last few decades, reliability-based methods have been applied to optimize structural design codes, which generally result to more rational and consistent reliability levels [14].

* Corresponding author.
E-mail address: joey@ramboll.com (J. Velarde).

https://doi.org/10.1016/j.engstruct.2020.111090
Received 2 December 2019; Received in revised form 8 May 2020; Accepted 6 July 2020

The procedure outlined in this section is based on the *Joint Committee on Structural Safety* (JCSS) [15] approach for calibration of safety factors.

2.1. Code calibration

Code calibration refers to the selection of code parameters to achieve a desired level of reliability. It is an optimization procedure, which requires both deterministic and probabilistic design approaches. A practical code calibration procedure can be summarized by the following steps [14,16]:

1. Define the scope of the code
2. Define the code objectives
3. Define the code format
4. Identify the typical failure modes and related stochastic models
5. Define a measure of closeness between code realization and its objective
6. Determine the optimal partial safety factors for the chosen code format
7. Verify the code and the partial safety factors

The (1) scope of the code refers to the class of the structure and critical failure modes to be considered, while the (2) objectives can be defined by the target reliability indices or target probabilities of failure (refer to Section 2.2). The (3) code format deals with the number of partial safety factors and load combination factors, if any. In some instances, re-writing of the code format is performed to reflect a more correct design philosophy, to align with other international standards, or to simplify code formulation [14]. Step (4) deals with the identification of the relevant failure modes and the corresponding design and limit state equations. The stochastic models representing the loads and resistance parameters are also defined, including statistical correlations. Recommendations related to stochastic modeling of load, resistance and model uncertainties can be found in the *JCSS Probabilistic Model Code* [15].

The partial safety factors $\gamma = [\gamma_1, \gamma_2, ..,\gamma_n]$ are calibrated considering $j = 1, 2, ..,L$ number of relevant failure modes. The measure of closeness defined in step (5), normally expressed as the square of the difference between the target reliability index (β_t) and the actual reliability index (β_j) for failure mode j, is included in a general optimization problem defined by Eq. (1).

$$\min_{\gamma} W(\gamma) = \sum_{j=1}^{L} w_j(\beta_j(\gamma) - \beta_t)^2 \tag{1}$$

where w_j is the weighting factor indicating the relative importance of design situation j. Based on Eq. (1), the optimal set partial safety factors (γ) can be obtained. It is noted that an alternative optimization problem can be formulated using probabilities of failure instead of reliability indices. The target reliability level could also be different for different failure modes, depending on the consequences of failure.

In step (6), the reliability index (β_j) is normally estimated by FORM/SORM [14] based on the limit state equations and stochastic parameters defined in Step (4). Note that the target reliability level is given with a reference period (typically 1 year). Lastly, the verification (step 7) involves taking into account engineering judgement, practical considerations and accummulated experience.

The scope of the calibration exercise demonstrated in this study considers a concrete GBF for offshore wind turbines. Failure of the concrete foundation due to fatigue damage accummulation is considered, following the DNV code [17] for *Offshore Concrete Structures*. Other relevant design codes for fatigue design of concrete structures, such as the *fib Model Code* [18] and *Eurocode (EN 1990)* [19] are based on a different design format that does not employ *FDF*. This study employs the DNV [17] format. The resistance model for concrete fatigue is further discussed in Section 5.

Table 1
Tentative target reliability levels related to one year reference period [15].

Relative cost of safety measure	Consequences of failure		
	Minor	Moderate	Large
Large	$\beta = 3.1 (P_F \approx 10^{-3})$	$\beta = 3.3 (P_F \approx 5{\cdot}10^{-4})$	$\beta = 3.7 (P_F \approx 10^{-4})$
Medium	$\beta = 3.7 (P_F \approx 10^{-4})$	$\beta = 4.2 (P_F \approx 10^{-5})$	$\beta = 4.4 (P_F \approx 5{\cdot}10^{-6})$
Small	$\beta = 4.2 (P_F \approx 10^{-5})$	$\beta = 4.4 (P_F \approx 5{\cdot}10^{-6})$	$\beta = 4.7 (P_F \approx 10^{-6})$

2.2. Target reliability level

The target reliability level has a direct influence on the recommended partial safety factors. For unmanned offshore wind turbines, the risk of fatality due to failure of a structural element is not significant. OWTs are therefore classified as having minor consequences of failure with large relative costs of safety measures. Based on Table 1 [15,20], a target reliability level corresponding to an annual probabilities of failure, $P_f = 10^{-3}$ to $5{\cdot}10^{-4}$ ($\beta = 3.1 - 3.3$), are normally used in developing design rules for OWTs [21–23]. This value can vary depending on the possibility of inspection and repair, and on the consequence of fatigue failure (e.g. due to structural redundancy).

2.3. Calibration approach

For fatigue design of offshore steel structures, partial safety factors related load (γ_f) and resistance (γ_Q) models are traditionally expressed in terms of *fatigue design factor*, which is the product of both partial safety factors ($FDF = \gamma_f \gamma_Q$). This is also commonly referred to as *design fatigue factor (DFF)*. The required FDF depends on the possibility of inspection, on the level of exposure and on whether the structural detail is a critical component. A range of *FDF* values from 1.5 to 3 for steel welded details are recommended by DNVGL [24].

For offshore concrete structures, fatigue design based on *FDF* has also been adapted, particularly in the DNVGL standard for offshore concrete structures [17]. In addition to safety margin provided by *FDF*, additional partial safety factor (γ_m) on the concrete material strength is recommended by the code. Proper calibration of these safety factors is essential for cost-effective foundations. A case study [25] on a concrete bridge showed that resistance partial safety factor for fatigue can be lowered without compromising fatigue reliability.

As shown in a previous study [26], the uncertainty related to the concrete fatigue damage model governs the fatigue reliability of OWT concrete structures. This suggests that calibration of material partial safety factor (γ_m) is more rational, and can lead to more profound effects than calibration of *FDF*. Fig. 1 illustrates the calibration approach performed in this study. Deterministic calculations are performed for a chosen design parameter $\mathbf{z}$. Based on the wind turbine design fatigue load and design resistance models, a set of design parameters ($\mathbf{z}^*$) corresponding to selected partial safety factors (γ_m, FDF) can be derived such that the design equation is satisfied ($G(x_d, \mathbf{z_i}) = 0$). Probabilistic analysis is then carried out using these design parameters to evaluate the reliability level. Finally, a set of material partial safety factors conditional to FDF ($\gamma_m|FDF$) are recommended based on how the code realizations ($\beta(\mathbf{z}^*)$) compare with the target reliability (β_t). The deterministic and probabilistic load and resistance models are discussed in the succeeding sections.

3. Uncertainties in fatigue design

Uncertainties can generally be classified into (1) aleatory or (2) epistemic uncertainties. Aleatory uncertainties refer to the physical or inherent randomness, which are found in environmental conditions and material properties. Epistemic uncertainties refer to having limited information or knowledge about a system, and covers statistical,

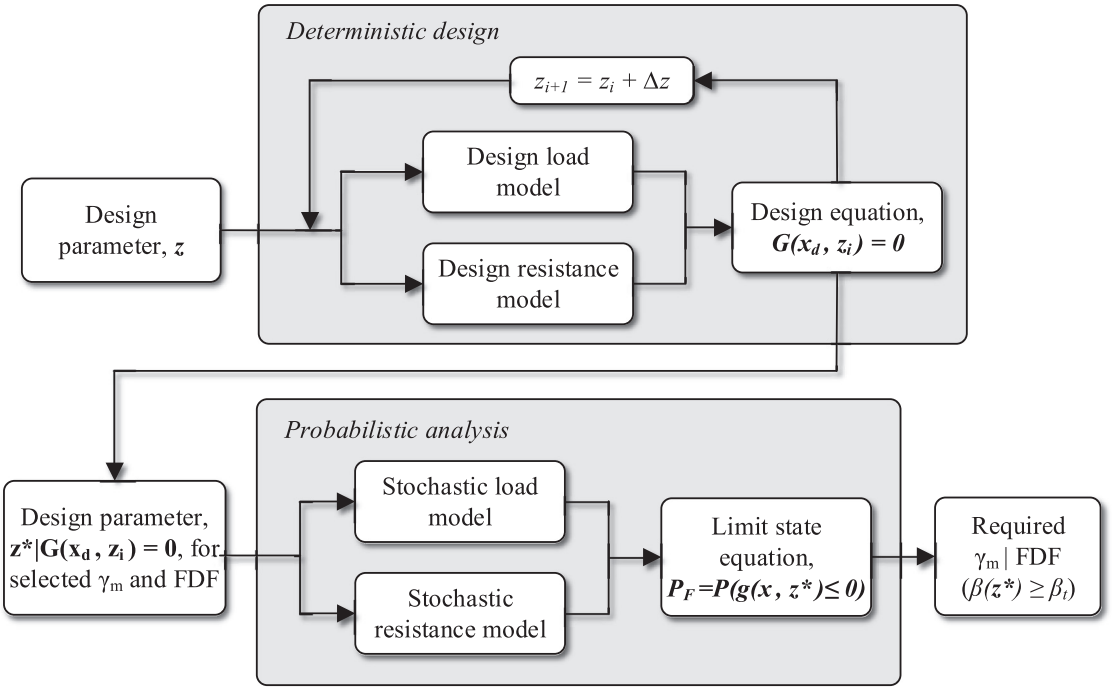

Fig. 1. Reliability-based approach for calibration of materal partial safety factor, γ_m.

measurement and model uncertainties. Unlike aleatory uncertainties, epistemic uncertainties can be further reduced by increasing the amount of data, improving the quality of data, or developing better mathematical models to describe a physical phenomena. Both aleatory and epistemic uncertainties need to be accounted for when calibrating partial safety factors [16,6].

Uncertainties are normally modelled by using stochastic parameters defined by a distribution function and distribution parameters. The *JCSS Probabilistic Model Code* [15] recommends probabilistic load and resistance models, which covers a wide range of practical engineering applications. For fatigue assessment of offshore wind turbines, general sources of uncertainty related to the loads include assessment of metocean conditions, aerodynamic models, hydrodynamic models, structural modelling and wind turbine control. On the fatigue resistance side, the primary sources of uncertainties include material fatigue strength and fatigue model—e.g., cumulative linear damage model or fracture mechanics model [4,15,27].

4. Wind turbine load effects

Current industry practice for estimation of offshore wind turbine responses is based on running an extensive set of time-domain simulations. A fully integrated OWT model is normally used, where aerodynamic loads, hydrodynamic loads, wind turbine control and soil-structure interaction are considered in each time step (Δt). A case of a concrete GBF is investigated in this study, where the fatigue reliability of the foundations is evaluated for both 5 MW and 10 MW reference wind turbine cases.

4.1. Case study: Thornton Bank GBF concept

The GBF concept based on the Thornton Bank offshore wind farm (Phase 1) considered in this study is shown in Fig. 2. The foundation is approximately 44 m high and has a 23.5 m base diameter, which tapers to 6.5 m diameter at the shaft. The post-tensioned reinforced concrete GBF is originally designed to support a 5 MW OWT at a mean water depth of 25 m in the North Sea. More information about the Thornton bank GBF concept can be found in [28,29].

Fig. 2. Thornton bank gravity-based foundation concept © C-Power.

4.2. Long-term metocean conditions

The assumed metocean conditions are based on the site characteristics of *Vesterhav Nord* offshore wind farm, which is located at the Danish North Sea. The long-term metocean condtions were generated from the Danish Meteorological Insitute's (DMI) hindcast models, which were validated against 11 years of available measurements. The representative mean wind speeds at hub height (U_{hub}) and turbulence intensities at different fractiles are summarized in Table 2. The U_{hub} is assumed to follow a Weibull distribution, with scale parameter, $A = 10.67$ m/s and shape parameter, $k = 2.23$.

Fatigue design loads are calculated using the characteristic value of the turbulence intensity TI_{90}, which is given by the 90% quantile of the turbulence standard deviation (σ_1) as shown in Eq. (2) and Eq. (3), respectively [21]. Design fatigue factors are calibrated based on the safety margin resulting from this design principle.

$$TI_{90} = \sigma_1 / U_{hub} \tag{2}$$

$$\sigma_1 = I_{ref}(0.75U_{hub} + b);\ b = 5.6\ \text{m/s} \tag{3}$$

For probabilic fatigue analysis, it is important to account for the

Table 2
Representative U_{hub} and turbulence intensities at different fractiles from wind farm data [30].

Sea state	Wind direction: 0 − 360deg	U_{hub} [m/s]	Occ. [-]	Turbulence Intensity [-]							
				Char.	Other fractiles						
				0.90	0.05	0.20	0.35	0.50	0.65	0.80	0.95
1	4–6	5	0.053	0.262	0.067	0.114	0.145	0.173	0.201	0.235	0.294
2	6–8	7	0.104	0.217	0.069	0.108	0.132	0.153	0.174	0.198	0.239
3	8–10	9	0.152	0.192	0.072	0.106	0.126	0.142	0.158	0.177	0.208
4	10–12	11	0.179	0.176	0.075	0.104	0.121	0.135	0.149	0.164	0.189
5	12–14	13	0.171	0.165	0.077	0.104	0.118	0.130	0.142	0.155	0.176
6	14–16	15	0.130	0.157	0.079	0.103	0.116	0.127	0.137	0.148	0.166
7	16–18	17	0.092	0.151	0.081	0.103	0.115	0.124	0.133	0.143	0.159
8	18–20	19	0.055	0.146	0.082	0.103	0.114	0.122	0.130	0.139	0.153
9	20–22	21	0.030	0.142	0.083	0.103	0.113	0.121	0.128	0.136	0.148
10	22–24	23	0.016	0.139	0.085	0.103	0.112	0.119	0.126	0.133	0.145
11	24–26	25	0.007	0.136	0.086	0.103	0.111	0.118	0.124	0.131	0.141
Total occ. [%]			**98.9**	-	12.5	15.0	15.0	15.0	15.0	15.0	12.5

turbulence intensity distribution to avoid hidden safety. A Weibull distribution (Eq. (4)) can be assumed for other turbulence standard deviation quantiles (σ_0), with scale (C) and shape (k) parameters defined by Eq. (5) and Eq. (6), respectively [21].

$$F(\sigma_0|U_{hub}) = 1 - \exp\left[-\left(\frac{\sigma_0}{C}\right)^k\right] \tag{4}$$

$$C = I_{ref}\,(0.75U_{hub} + 3.3\ \text{m/s}) \tag{5}$$

$$k = 0.27U_{hub} + 1.4 \tag{6}$$

The lumped representative sea states for fatigue analysis are summarized in Table 3, with the mean significant wave height (H_s) and mean wave period (T_p) derived from wind and wave correlation. Based on the global sensitivity analysis [31] performed on the same case study, it can be assumed that the variation in the predicted fatigue loads is governed by the uncertainty related to the turbulence intensity. For simplicity, the effects of wind and wave directionality are ignored.

4.3. Wind turbine load model

The aeroelastic simulation tool, *HAWC2* [32], is used to develop the OWT integrated models where both wind and wave loads are included. *HAWC2* is based on a multibody formulation, where each structural component is modelled by Timoshenko beam elements with six degrees of freedom (6 DOF), x. For a given mass matrix $[M]$, damping matrix $[D]$ and stiffness matrix $[K]$ representing the OWT, the general equation of motion can be written as shown in Eq. (7).

Table 3
Representative sea states for fatigue analysis based on wind farm data [30].

Sea state	U_{hub} range	$U_{hub}\,[m/s]$	Occ. [-]	Mean $H_s\,[m]$	Mean $T_p\,[s]$
1	4–6	5	0.053	0.82	6.8
2	6–8	7	0.104	1.01	7.0
3	8–10	9	0.152	1.24	7.1
4	10–12	11	0.179	1.55	7.4
5	12–14	13	0.171	2.01	7.8
6	14–16	15	0.130	2.53	8.2
7	16–18	17	0.092	3.07	8.9
8	18–20	19	0.055	3.65	9.9
9	20–22	21	0.030	4.08	10.4
10	22–24	23	0.016	4.76	11.4
11	24–26	25	0.007	5.40	12.9
Sum			**0.989**		

$$[M]\ddot{x} + [D]\dot{x} + [K]x = F_{aero} + F_{hydro} \tag{7}$$

where F_{aero} and F_{hydro} are the aerodynamic and hydrodynamic forces, respectively.

The *HAWC2* model of the Thornton bank GBF supporting a 5 MW reference wind turbine is illustrated in Fig. 3. A combined soil and structural damping ratio, $\zeta_{soil+struc} = 1\%$, is assumed for the first fore-aft and side-side modes. In addition, the aerodynamic and hydrodynamic damping contributions are also considered in the simulations based on the wind and wave input parameters, respectively. Table 4 summarizes the key elevations and reference wind turbine properties used in the simulations.

For all wind conditions summarized in Table 2, turbulent wind fields were generated based on the *Mann* turbulence model [35]. The Normal Turbulence Model (NTM) [22] is assumed for fatigue analysis. Based on metocean data, metocean data, a power law wind profile is assumed with a shear exponent, $\alpha = 0.08$ (0.14 for characteristic fatigue load). The aerodynamic loads (F_{aero}) were calculated based on the *Blade Element Momentum* (BEM) theory [36,37].

For all sea states summarized in Table 3, linear irregular waves were generated based on the JONSWAP spectrum. The hydrodynamic loads (F_{hydro}) were calculated based on Morsion's equation [38], where the total force per unit length is defined as the sum of the drag and inertia components. Both load components can be expressed as a function of water density (ρ), sectional area (A), and wave particle velocity (U) and

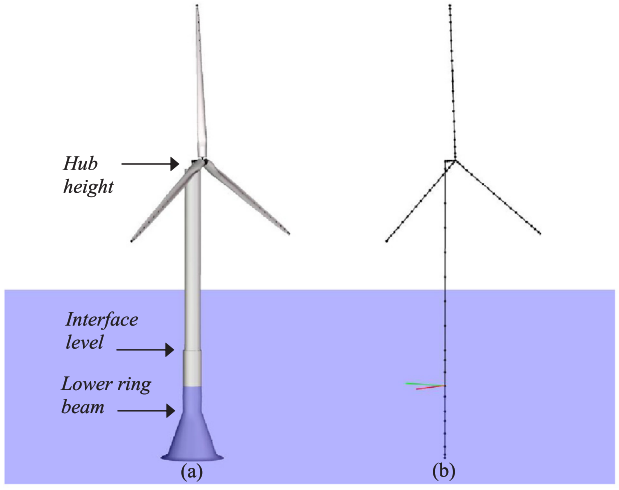

Fig. 3. *HAWC2* model of a GBF supporting a 5 MW reference wind turbine: (a) surface model; (b) beam elements.

Table 4
Key elevations and reference wind turbine properties [33,34].

Parameter	NREL 5 MW	DTU 10 MW
Rating [MW]	5	10
Rotor diameter [m]	126	178.3
Number of blades [–]	3	3
Cut-in, rated, cut-out U_w [m/s]	3.0, 11.4, 25.0	4.0, 11.4, 25.0
Dynamic rotor speed range [rpm]	6.9, 12.1	6.0, 9.6
Hub height [m]	91.7	114
Interface elevation [m]	14.7	14.7
Mean water depth [m]	25	25

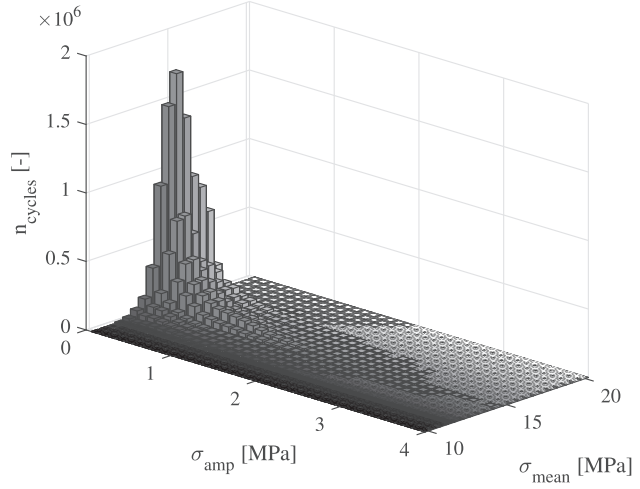

Fig. 4. Markov matrix showing annual number of cycles for probabilistic analysis (5 MW OWT) accounting for wind speed and turbulence intensity distribution.

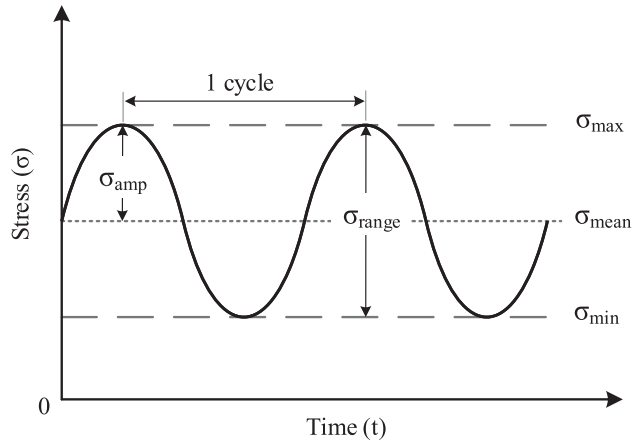

Fig. 5. Defintion of a stress cycle mean, amplitude and range.

acceleration ($\dot{U}$) as defined by Eq. (8). The drag (C_D) and inertia (C_M) coefficients were calibrated to account for diffraction and secondary steel.

$$F_{hydro} = \rho C_D D U|U| + \rho C_M A \dot{U} \tag{8}$$

Based on modified IEC [22] design load cases (DLC), time-domain fatigue simulations covering power production (DLC 1.2) and idling situations (DLC 6.4) were performed. Each simulation corresponding to the sea states defined in Table 2 and Table 3 has a 10- minutes duration and six independent realizations. The loads are scaled assuming a 95% wind turbine availability and 25 years of design lifetime. For simplicity, wind and wave misalignment is considered not important for this study,

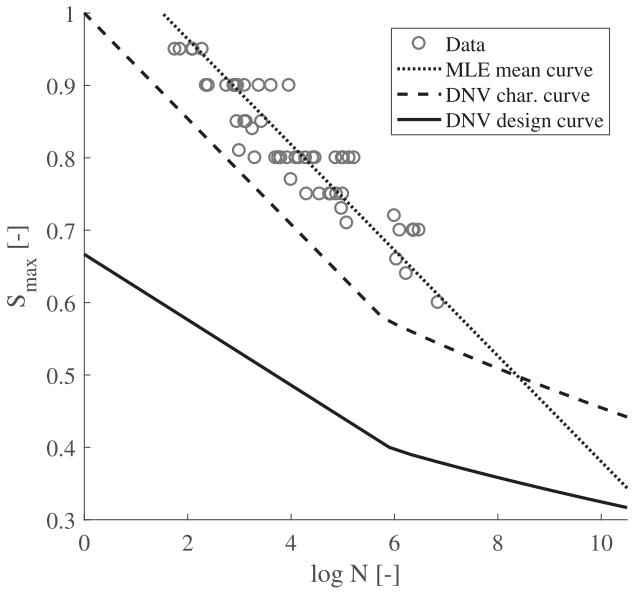

Fig. 6. Concrete S-N curve based on available fatigue tests ($S_{min} = 0.12$) and DNV code [17]. All curves are plotted against $S_{max} = \sigma_{max}/f_c$.

and thus unidirectional loading is assumed for both 5 MW and 10 MW cases.

The resulting load time histories are used to estimate the stresses at a critical concrete section. The lower ring beam, located at 14.5 m above the mudline (see Fig. 3), is assumed to be most critical. Using a standard rainflow count algorithm, the number of load cycles for predefined stress bins are derived. Fig. 4 shows the distribution of load cycles (n_{cycles}) according to the mean stress (σ_{mean}) and stress amplitude (σ_{amp}), which is also referred to as the *Markov* matrix. The *Markov* matrices are evaluated together with the design and probabilistic fatigue resistance models, which are presented in the next section.

5. Concrete fatigue reliability model

During code optimization, it is important to account for the hidden safety margins included in the code format. The following fatigue resistance model formulations are based on recommendations in the DNV standard for *Offshore Concrete Structures* [17].

5.1. Deterministic design

A cumulative linear damage theory [39,40] is assumed for fatigue assessment. Given the number of stress cycles ($n_{i,j,k}$) and the corresponding number of cycles to failure ($N_{j,k}$) in each sea state bin i, mean stress bin j and stress amplitude bin k, the damage can be quantified by integrating over the total number of representative sea states (N_{U_w}), mean stress bins ($N_{\sigma_{mean}}$) and stress amplitude bins ($N_{\sigma_{amp}}$) . The design equation can be written as shown in Eq. (9). A *Markov* matrix is obtained for each sea state, which is defined according to the mean wind speed (U_w) distribution.

$$G(t, \mathbf{z}) = 1 - \sum_{i=1}^{N_{Uw}} \sum_{j=1}^{N_{\sigma mean}} \sum_{k=1}^{N_{\sigma amp}} \frac{n^d_{i,j,k} p_i FDFT_L}{N^d_{j,k}} = 0 \tag{9}$$

where:

$n^d_{i,j,k}$ is the design number of stress cycles per year at bin i, j, k.
$N^d_{j,k}$ is the number of stress cycles to failure at stress bin j, k calculated from the design resistance as a function of the material partial safety factor (γ_m).
p_i is the occurrence probability of design sea state i ($\sum p_i = 1$).
T_L is the design lifetime (25 years)

Table 5
Stochastic model parameters for the concrete fatigue; LN: LogNormal; N: Normal; Values inside () applies for the 10 MW case.

Parameter	Distribution	Mean	Std.	Remark	Reference
Δ	LN	1.00	0.30	Linear damage accummulation model uncertainty	[45,46]
X_{S1}	LN	1.00	0.10	Load amplitude uncertainty	[46]
X_{S2}	LN	1.00	0.10	Mean load uncertainty	[46]
X_{dyn}	LN	1.00	0.05 (0.10)	Dynamic response uncertainty	[6]
X_{stress}	LN	1.00	0.05	Stress calculation uncertainty	[6]
X_{fc}	LN	1.00	0.14	Concrete compressive strength uncertainty	[15]
X_m	N	1.52	0.75	Resistance model uncertainty estimated from data	[26]

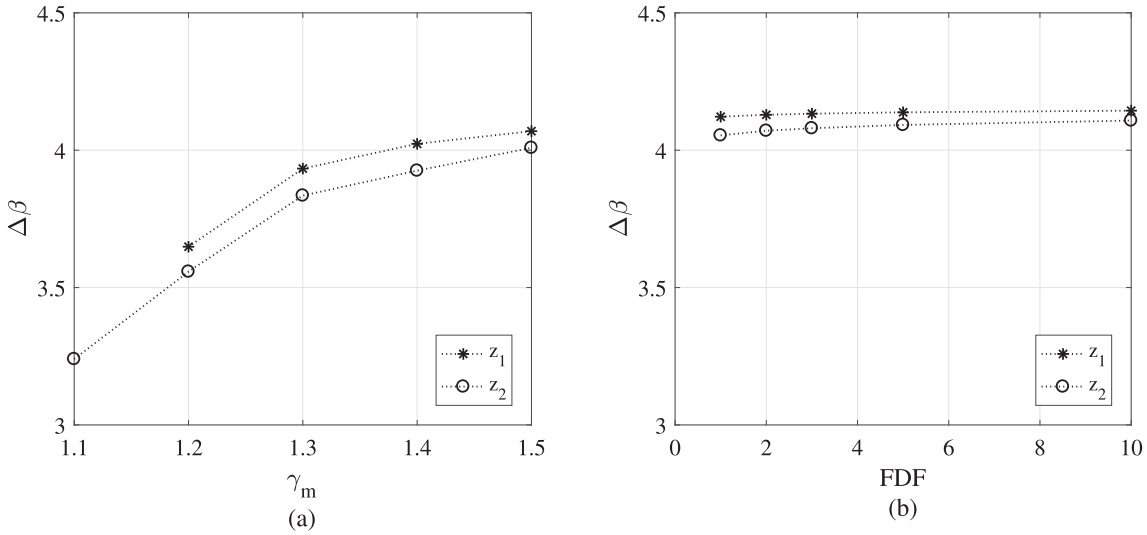

Fig. 7. Calculated annual reliability index ($\Delta\beta$) for the 5 MW case as a function of (a) material partial safety factor, γ_m ($FDF = 3$) and (b) FDF ($\gamma_m = 1.5$) given design parameters z_1 and z_2.

In addition to the stress cycle amplitude, the mean stress is an important parameter in defining the concrete resistance against fatigue. The S-N curves for concrete are normally expressed in terms of the maximum (σ_{max}) and minimum (σ_{min}) compressive stress within each stress block, which are calculated from the mean (σ_{mean}) and amplitude (σ_{amp}) of each stress cycle as illustrated in Fig. 5. Both σ_{max} and σ_{min} are obtained from the *Markov* matrix.

The design number of cycles to failure ($N^d_{j,k}$), with superscript *"d"* indicating design value, is calculated based on Eq. (10). The factor $C_1 = 10$ for structures in water having stress variation in the compression-compression range is used, while the fatigue strength parameter $C_5 = 1$ for concrete [17]. If the calculated design life ($\log_{10}N^d$) is greater than X^d, this value can be increased by a factor C_2^d. The parameters X^d and C_2^d are expressed as shown in Eq. (11) and Eq. (12), respectively.

$$\log_{10}N^d = \begin{cases} C_1 \dfrac{1-\frac{\sigma_{max}}{C_5 f_{rd}}}{1-\frac{\sigma_{min}}{C_5 f_{rd}}}, & \log_{10}N^d \leqslant X^d. \\ C_1 C_2^d \dfrac{1-\frac{\sigma_{max}}{C_5 f_{rd}}}{1-\frac{\sigma_{min}}{C_5 f_{rd}}}, & \log_{10}N^d > X^d. \end{cases} \tag{10}$$

$$X^d = \frac{C_1}{1-\frac{\sigma_{min}}{C_1 f_{rd}+0.1C_1}} \tag{11}$$

$$C_2 = (1 + 0.2(\log_{10}N^d - X)) > 1.0 \tag{12}$$

The design fatigue compressive strength (f_{rd} [MPa]) is related to the characteristic compressive cylinder strength(f_{cck} [MPa]) by Eq. (13), where $\alpha = 1$ for concrete in compression. Eq. (13) is valid for concrete grades C25 to C90 [17]. Assuming a C45 concrete grade with $f_{cck} = 45$ MPa and using a recommended material partial safety factor of $\gamma_m = 1.50$ for concrete fatigue, $f_{rd} \approx 27.75$ MPa.

$$f_{rd} = \alpha \frac{f_{cck}(1 - f_{cck}/600)}{\gamma_m} \tag{13}$$

Concrete design S-N curves are normally expressed as a function of S^d_{max} and S^d_{min}, which are equivalent to the σ_{max} and σ_{min} normalized to the design compressive strength f_{rd} as shown in Eq. (14). The design S-N curve is illustrated in Fig. 6, which also shows the design code safety margin relative to the mean and characteristic curves. The mean curve is derived based the Maximum Likelohood Method (MLM), applied on a database of experimental fatigue tests [41–44]. In particular, test results with $S_{max} \geqslant 0.6$ covering $f_{cck} = 20$ to $60MPa$ are considered in the MLM fit.

$$S^d_{max} = \frac{\sigma_{max}}{C_5 f_{rd}}, \quad S^d_{min} = \frac{\sigma_{min}}{C_5 f_{rd}} \tag{14}$$

Creep, shrinkage and size effects are not considered in design load calculation, since these effects are not covered by the fatigue test results. The probabilistic analysis covers the uncertainty related to the linear damage accummulation model. In addition, fatigue tests used to evaluate the uncertainty were performed under in-air conditions. For simplicity, the same level of uncertainty is assumed for both air and seawater exposures. The factor C_1 in Eq. (10) adapts the curve for either in-air ($C_1 = 12$) or seawater ($C_1 = 10$) conditions.

5.2. Probabilistic design

The limit state equation for fatigue failure of concrete is written as shown in Eq. (15). The resistance is represented by the stochastic parameter Δ, which represents the Miner's rule (linear damage accummulation) model uncertainty. In addition to the wind speed (U_w) distribution, the load model also accounts for the statistical distribution of turbulence intensity (TI), which is the governing source of load

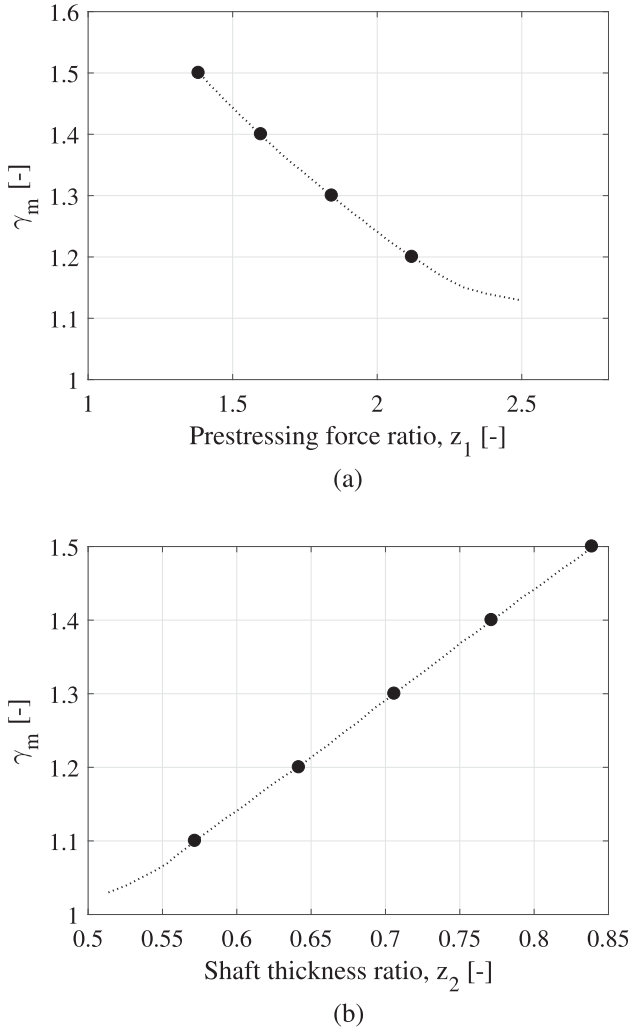

Fig. 8. Relationship between material partial safety factor (γ_m) and design parameters (a) z_1 (with $z_2 = 1.0$) and (b) z_2 (with $z_1 = 1.0$) for a 5 MW offshore wind turbine.

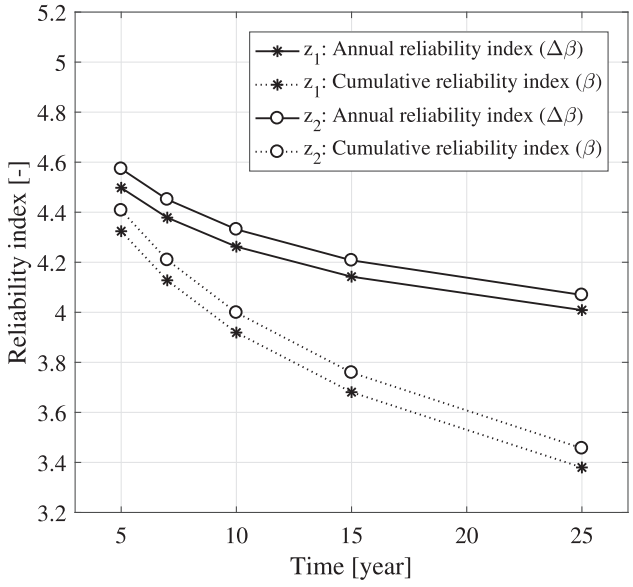

Fig. 9. Reliability indices ($\Delta\beta$, β) for z_1 (with $z_2 = 1.0$) and z_2 (with $z_1 = 1.0$) for the 5 MW case as a function of service life ($\gamma_m = 1.5$).

Table 6
Annual reliability index ($\Delta\beta$) for different combinations of material partial safety factor (γ_m) and design parameters (z_1, z_2) conditional to $FDF = 3$ for a 5 MW OWT.

γ_m [−]	Prestressing force		Shaft thickness		$\Delta\beta$
	z_1	F_{PT} [MN]	z_2	t [mm]	
1.1	-	-	-	-	-
1.2	2.12	197	1.00	500	3.65
1.3	1.84	171	1.00	500	3.93
1.4	1.60	149	1.00	500	4.02
1.5	1.38	129	1.00	500	4.07
1.1	1.00	93	0.57	286	3.24
1.2	1.00	93	0.64	321	3.56
1.3	1.00	93	0.71	353	3.83
1.4	1.00	93	0.77	386	3.93
1.5	1.00	93	0.84	419	4.01

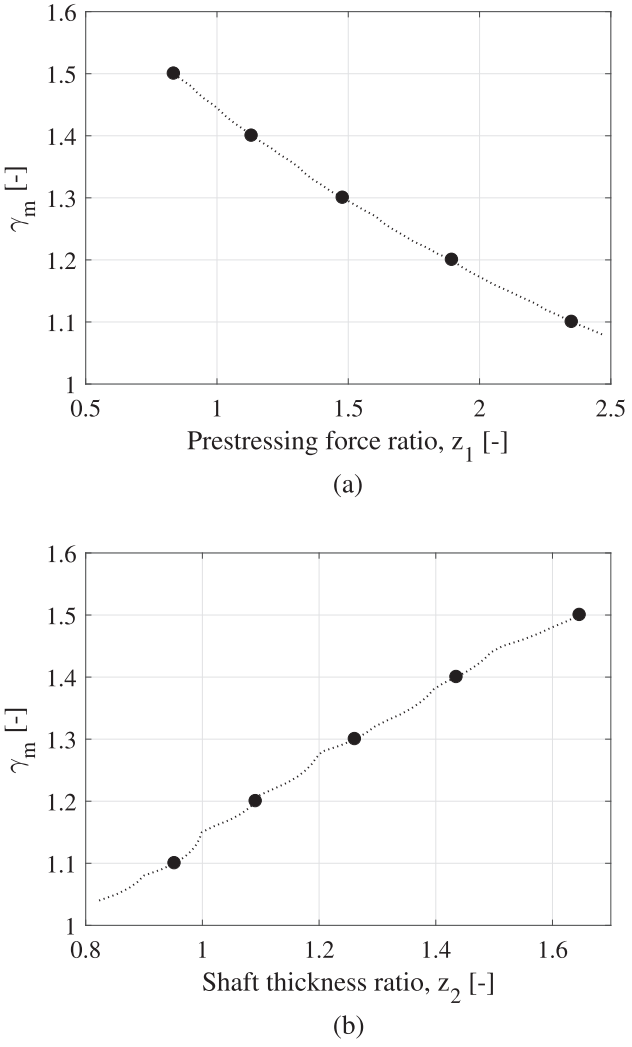

Fig. 10. Relationship between material partial safety factor (γ_m) and design parameters (a) z_1 (with $z_2 = 1.5$) and (b) z_2 (with $z_1 = 1.0$) for a 10 MW reference case.

uncertainty during power production [31]. It is assumed that the uncertainty in the calculated number of cycles ($n_{i,j,k}$) is relatively small.

$$g(\mathbf{z}, t) = \Delta - \sum_{i=1}^{N_{U_w,TI}} \sum_{j=1}^{N_{\sigma mean}} \sum_{k=1}^{N_{\sigma amp}} \frac{n_{i,j,k} p_i t}{N_{j,k}} \tag{15}$$

where:

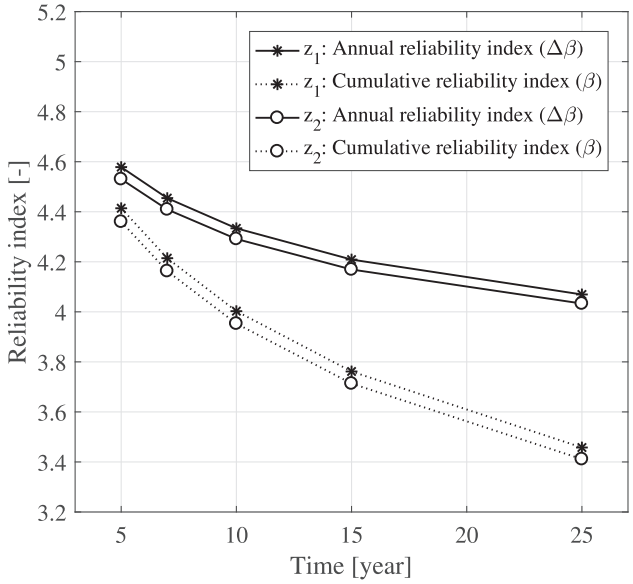

Fig. 11. Reliability indices ($\Delta\beta$, β) for z_1 (with $z_2 = 1.0$) and z_2 (with $z_1 = 1.0$) for the 10 MW case as a function of service life ($\gamma_m = 1.5$).

Table 7
Annual reliability index ($\Delta\beta$) for different combinations of material partial safety factor (γ_m) and design parameters (z_1, z_2) conditional to $FDF = 3$ for a 10 MW OWT.

γ_m[−]	Prestressing force		Shaft thickness		$\Delta\beta$
	z_1	F_{PT}[MN]	z_2	t[mm]	
1.1	2.35	219	1.50	750	3.31
1.2	1.90	176	1.50	750	3.58
1.3	1.48	138	1.50	750	3.87
1.4	1.13	105	1.50	750	3.99
1.5	0.84	78	1.50	750	4.03
1.1	1.00	93	0.95	476	3.08
1.2	1.00	93	1.09	546	3.38
1.3	1.00	93	1.26	631	3.76
1.4	1.00	93	1.44	718	3.98
1.5	1.00	93	1.65	823	4.07

Table 8
Reduction in shaft thickness (%) and reliability index ($\Delta\beta$) as a function of material partial safety factor (γ_m) for both 5 MW and 10 MW cases (considering FLS only).

γ_m	5 MW		10 MW	
	Reduction [%]	$\Delta\beta$	Reduction [%]	$\Delta\beta$
1.1	31.8	3.24	42.2	3.08
1.2	23.5	3.56	33.7	3.38
1.3	15.8	3.83	23.4	3.76
1.4	8.0	3.93	12.8	3.98
1.5	0.0	4.01	0.0	4.07

$n_{i,j,k}$ is the number of stress cycles per year at bin i, j, k.
p_i is the occurrence probability of wind speed and turbulence intensity($\sum p_i = 1$).
t is the time in years ($0 < t \leqslant T_L$).

The uncertain parameters in the fatigue resistance model are represented by stochastic variables. Following the same equations used in the design, the number of stress cycles to failure (N) is calculated using Eqs. (16)–(19). In general, predictions of stress amplitudes have higher uncertainties compared to the mean stress estimates. This is accounted for by separately modelling the uncertainties for both mean and amplitude stress components as shown in Eq. (18) and Eq. (19). It is noted that the mean S-N curve illustrated in Fig. 6) is defined without accounting for the asymptotic second slope at the lower maximum stress ranges ($S_{max} < 0.6$) due to lack of experimental tests covering lower stress cycle fatigue supporting this assumption.

$$\log_{10}N = C_1\frac{1-\frac{\sigma_{max}}{C_5 f_{ns}}}{1-\frac{\sigma_{min}}{C_5 f_{ns}}} + X_m \tag{16}$$

$$f_{ns} = X_{fc} f_{cm}(1 - X_{fc} f_{cm}/600) \tag{17}$$

$$\sigma_{max} = X_{S2}X_{stress}\sigma_{mean} + X_{S1}X_{stress}X_{dyn}\sigma_{amp} \tag{18}$$

$$\sigma_{min} = X_{S2}X_{stress}\sigma_{mean} - X_{S1}X_{stress}X_{dyn}\sigma_{amp} \tag{19}$$

where:

X_m models the resistance model uncertainty related to concrete S-N curve.
X_{fc} models the concrete strength uncertainty.
f_{cm} models the mean static compressive strength in MPa
f_{ns} models the stochastic in situ compressive strength in MPa
X_{S1} models the load model uncertainty related to the amplitude stress (σ_{amp}).
X_{S2} models the load model uncertainty related to the mean stress (σ_{mean}).
X_{stress} models the uncertainty related to the stress calculation.
X_{dyn} models the uncertainty related to the dynamic response.

5.3. Reliability assessment

The limit state equation (Eq. (15)) involves the stochastic parameters summarized in Table 5. It is possible that a correlation exists between the load uncertainties X_{S1} and X_{S2}. Statistical indepence is assumed in this case study since the uncertainty sources for the mean stress (driven by prestressing) and the stress range (driven by wind and wave loads) can be considered partly independent.

Based on Eq. (15), the accumulated probability of failure at time t, $P_F(\mathbf{z}, t) = P(g(\mathbf{z}, t) \leqslant 0)$, is estimated using First Order Reliability Method (FORM) [14]. Hence, the corresponding reliability index can be estimated as $\beta(\mathbf{z}, t) = -\Phi^{-1}(P_F(\mathbf{z}, t))$, where Φ is the standard normal distribution function. The annual probability of failure (ΔP_F) and annual reliability index ($\Delta\beta$) is obtained by Eq. (20) and Eq. (21), respectively.

$$\Delta P_F(\mathbf{z}, t) = \frac{P_F(\mathbf{z}, t + \Delta t) - P_F(\mathbf{z}, t)}{(1 - P_F(\mathbf{z}, t))\Delta t} \tag{20}$$

$$\Delta\beta(\mathbf{z}, t) = -\Phi^{-1}(\Delta P_F(\mathbf{z}, t)) \tag{21}$$

where $t > \Delta t$ and Δt is the time interval taken as 1 year.

This study investigates two design parameters, namely the prestressing force (F_{PT}) and concrete shaft thickness (t). For simplicity, these parameters are expressed in terms of the ratio of the design parameter value to the default value of prestressing force (z_1) and shaft thickness (z_2) based on the Thornton bank GBF design. Based on the reliability-based calibration approach illustrated in Fig. 1, a relationship between selected safety factors (γ_m, FDF), design parameters (z_1, z_2) and fatigue reliabilty can be derived using the same design equation (Eq. (9)).

6. Numerical examples

The results summarized in this section only considers fatigue failure mode. In addition, no system effects are taken into account. A minimum $\Delta\beta = 3.1 (P_F \approxeq 10^{-3})$ is assumed acceptable for design of OWT support structures.

Table 9
Sensitivity factors (α_i^2) of stochastic input parameters for the 5 MW case at different values of design parameters, $z_1|\gamma_m$ and $z_2|\gamma_m$.

Parameter	Prestressing force ratio, $z_1\|\gamma_m$				Shaft thickness ratio, $z_2\|\gamma_m$				
	1.2	1.3	1.4	1.5	1.1	1.2	1.3	1.4	1.5
Δ	0.002	0.003	0.029	0.030	0.004	0.005	0.007	0.028	0.030
X_{S1}	0.013	0.017	0.008	0.004	0.030	0.032	0.035	0.013	0.006
X_{S2}	0.235	0.216	0.007	0.002	0.171	0.157	0.137	0.009	0.003
X_{fc}	0.599	0.592	0.047	0.020	0.567	0.551	0.520	0.072	0.027
X_{stress}	0.091	0.089	0.007	0.003	0.086	0.083	0.078	0.011	0.004
X_{dyn}	0.003	0.004	0.002	0.001	0.007	0.008	0.009	0.003	0.002
X_m	0.057	0.079	0.901	0.939	0.134	0.164	0.215	0.864	0.929
$\sum_{i=1}\alpha_i^2$	1.000	1.000	1.000	1.000	1.000	1.000	1.000	1.000	1.000

Table 10
Sensitivity factors (α_i^2) of stochastic input parameters for the 10 MW case at different values of design parameters, $z_1|\gamma_m$ and $z_2|\gamma_m$.

Parameter	Prestressing force ratio, $z_1\|\gamma_m$					Shaft thickness ratio, $z_2\|\gamma_m$				
	1.1	1.2	1.3	1.4	1.5	1.1	1.2	1.3	1.4	1.5
Δ	0.003	0.004	0.006	0.029	0.030	0.005	0.006	0.007	0.028	0.031
X_{S1}	0.025	0.032	0.040	0.012	0.006	0.041	0.046	0.049	0.013	0.004
X_{S2}	0.194	0.169	0.136	0.005	0.001	0.145	0.129	0.110	0.006	0.001
X_{fc}	0.592	0.579	0.546	0.055	0.021	0.561	0.545	0.514	0.060	0.014
X_{stress}	0.090	0.087	0.082	0.009	0.003	0.086	0.082	0.077	0.009	0.002
X_{dyn}	0.006	0.008	0.010	0.003	0.001	0.010	0.011	0.012	0.003	0.001
X_m	0.089	0.121	0.180	0.887	0.937	0.152	0.181	0.230	0.880	0.947
$\sum_{i=1}\alpha_i^2$	1.000	1.000	1.000	1.000	1.000	1.000	1.000	1.000	1.000	1.000

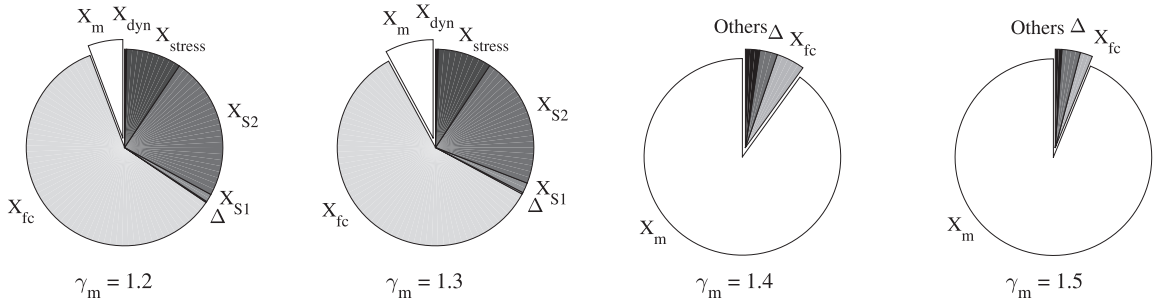

Fig. 12. Sensitivity (α_i^2) of fatigue reliability ($\Delta\beta$) to stochastic input parameters for the 5 MW case at different values of design parameter, $z_1|\gamma_m$ = 1.2, 1.3, 1.4, 1.5.

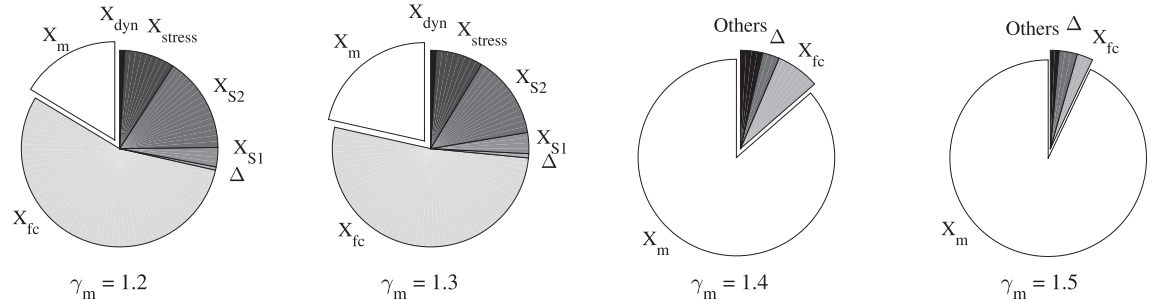

Fig. 13. Sensitivity (α_i^2) of fatigue reliability ($\Delta\beta$) to stochastic input parameters for the 5 MW case at different values of design parameter, $z_2|\gamma_m$ = 1.2, 1.3, 1.4, 1.5.

6.1. Comparison between γ_m and FDF

The fatigue design equation is formulated with two safety factors, namely the material partial safety factor (γ_m) and fatigue design factor (*FDF*). Based on the 5 MW OWT case study, an investigation of how variations in both γ_m and *FDF* affects the annual reliability index ($\Delta\beta$) is illustrated in Fig. 7.

For both design parameters, z_1 and z_2, a higher sensitivity on $\Delta\beta$ is observed for variations in γ_m conditional to *FDF* = 3. Alternatively, it can be concluded that the design parameters are not sensitive to changes in *FDF* conditional to fixed γ_m = 1.5.

The sensitivity analyses presented in the following sections verify that the uncertainties related to the material resistance model have the highest influence on the fatigue reliability. Hence the following investigation of fatigue reliability is performed for different values of γ_m conditional to *FDF* = 3.

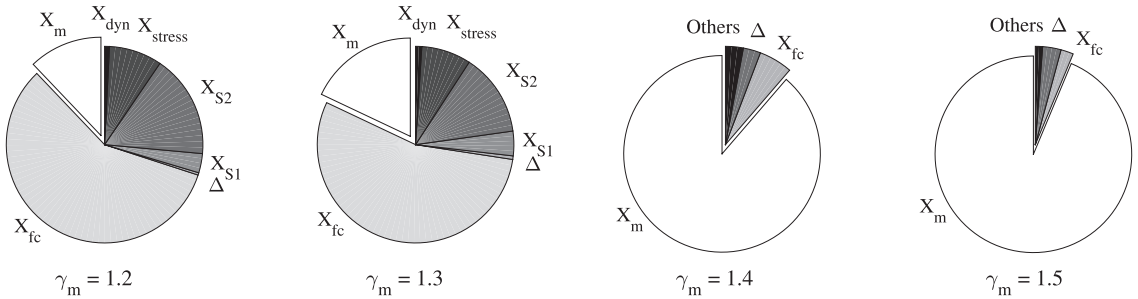

Fig. 14. Sensitivity (α_i^2) of fatigue reliability ($\Delta\beta$) to stochastic input parameters for the 10 MW case at different values of design parameter, $z_1|\gamma_m$ = 1.2, 1.3, 1.4, 1.5.

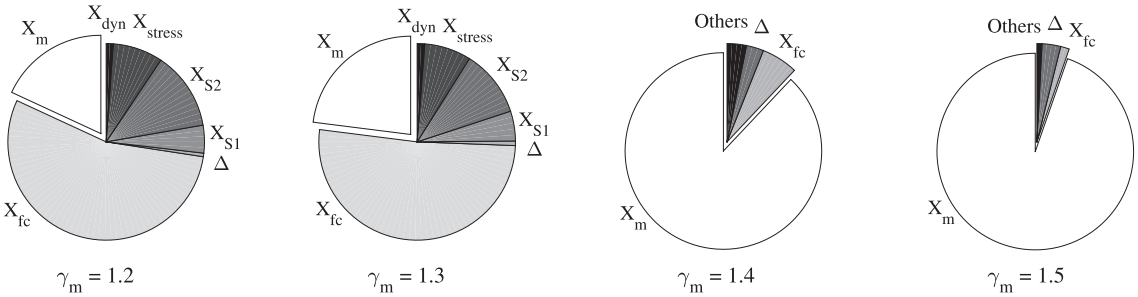

Fig. 15. Sensitivity (α_i^2) of fatigue reliability ($\Delta\beta$) to stochastic input parameters for the 10 MW case at different values of design parameter, $z_2|\gamma_m$ = 1.2, 1.3, 1.4, 1.5.

Table 11
Calculated sensitivity factors (α_i^2) of stochastic input parameters assuming X_{mCOV} = 0.50($\Delta\beta$ = 4.01) and X_{mCOV} = 0.25($\Delta\beta$ = 4.72).

Sensitivity ranking	X_{mCOV} = 0.50		X_{mCOV} = 0.25	
	Parameter	α_i^2	Parameter	α_i^2
1	X_m	0.9294	X_{fc}	0.6409
2	Δ	0.0300	X_{S2}	0.2024
3	X_{fc}	0.0265	X_{stress}	0.0941
4	X_{S1}	0.0059	X_{S1}	0.0264
5	X_{stress}	0.0041	X_m	0.0261
6	X_{S2}	0.0026	X_{dyn}	0.0066
7	X_{dyn}	0.0015	Δ	0.0034
$\sum \alpha_i^2$		1.00		1.00

6.2. Example 1: 5 MW offshore wind turbine

Using the design equation (Eq. (9)), relationships between material partial safety factor (γ_m) and design parameters z_1 and z_2 are derived as shown in Fig. 8a and Fig. 8b, respectively. The relation between γ_m and z_1 is derived for a fixed value of z_2 = 1.0, and vice versa. A lower γ_m allows for higher prestressing force, which is directly related to the mean stress on the concrete section. Similarly, a lower γ_m results to a decrease in the required concrete shaft thickness. The derived relationship only considers concrete fatigue safety.

The reliability indices are calculated based on the relationship between γ_m and design parameters ($z_1 z_2$). Fig. 9 illustrates the reliability indices as a function of service life in years. The $\Delta\beta$ at end of a 25-year service life are calculated and summarized in Table 6. All design combinations resulted in acceptable $\Delta\beta \geqslant 3.1$. The results of the reliability analysis indicates that a higher prestressing force (lower γ_m) can be applied on the section if necessary for design optimization. For design parameter z_2, results indicate that the shaft thickness of the original concept design can be reduced without compromising fatigue safety.

6.3. Example 2: 10 MW offshore wind turbine

Numerical Example 2 considers the same GBF concept to support a 10 MW offshore wind turbine. Fig. 10a and Fig. 10b show the derived relationships between γ_m and design parameters z_1 and z_2, respectively,

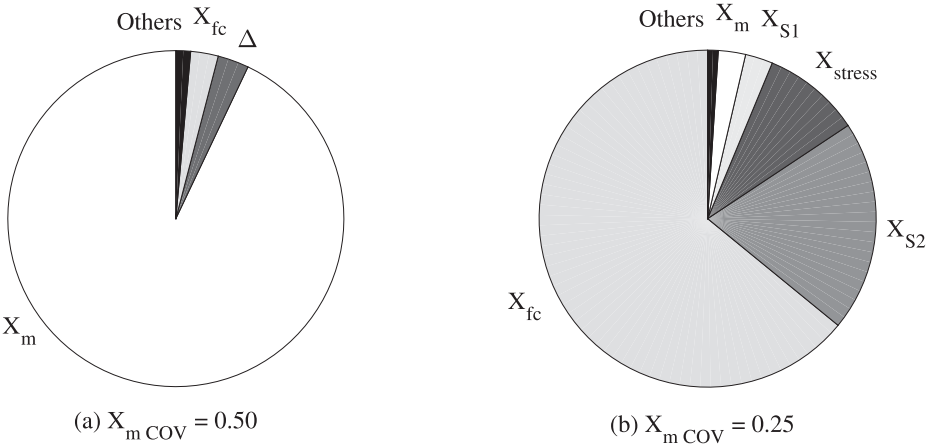

Fig. 16. Sensitivity (α_i^2) of fatigue reliability ($\Delta\beta$) to stochastic input parameters assuming (a) X_{mCOV} = 0.50 and (b) (*b*)X_{mCOV} = 0.25 for γ_m = 1.5 (z_1 = 1.0, z_2 = 0.84).

following the same trend as Example 1. To accommodate higher mean and amplitude loads and to satisfy the design equation at different values of z_1, the shaft thickness is increased by 50% ($z_2 = 1.5$). The same amount of prestressing force ($z_1 = 1.0$) can be assumed for variations in design parameter z_2.

The resulting reliability indices as a function of service life in years are shown in Fig. 11. The $\Delta\beta$ at end of a 25-year service life are calculated and summarized in Table 7. All design combinations resulted in acceptable $\Delta\beta \geqslant 3.1$, except for the design configuration with $\gamma_m = 1.1$, $z_1 = 1.00$ and $z_2 = 0.95$. The results indicate that the same GBF concept initially design for a 5 MW OWT can be used to support a 10 MW OWT, with minor modifications in design parameters. Similar to Example 1, it can also be concluded that a lower γ_m can be recommended without compromising fatigue safety, even for large wind turbines whose support structure design can be driven by fatigue.

6.4. Proposed material safety factor (γ_m)

The DNV standard for *Offshore Concrete Structures* [17] currently recommends a $\gamma_m = 1.5$. Table 8 summarizes the corresponding reduction in concrete shaft thickness and $\Delta\beta$ as a function of γ_m, considering FLS only. Results from both 5 MW case and 10 MW case indicate that a lower value of $\gamma_m = 1.1$ to 1.2 can be used, which potentially leads to significant reduction in the required structural dimensions while at the same time satisfying the required safety level ($\Delta\beta \geqslant 3.1$).

The presented results only considers the fatigue limit state. Thus, recommendation of a lower material safety factor (γ_m) can specifically benefit design situations where concrete foundation design is driven by FLS, as in the case of large offshore wind turbines ($\geqslant$10 MW). This reduction can significantly lead to an optimal concrete foundation design.

6.5. Sensitivity to input parameters

The sensitivity of the reliability index (β) to each stochastic input parameters (X_i) can be expressed in terms of the alpha factors (α_i) as defined in Eq. (22) [14]. The alpha factors, also referred to as *sensitivity factors*, are determined by FORM. When evaluated at the design point ($\mathbf{X}^*$), the relative importance can be obtained based on the definition $\sum_{i=1} \alpha_i^2 = 1$. Table 9 and Table 10 summarize the calculated α_i^2 factors for both 5 MW and 10 MW offshore wind turbine cases, respectively.

$$\alpha_i = \frac{\delta\beta}{\delta X_i} \tag{22}$$

The relative importance of stochastic parameters vary according to the assumed γ_m and correspoding design parameters. In general, the uncertainty related to concrete compressive strength (X_{fc}) is the governing parameter at lower γ_m values ($\gamma_m = 1.1, 1.2, 1.3$). These are associated with design configurations with high prestressing force or low shaft thickness, where the most likely fatigue failure is due to the relatively high mean stresses that result to lower resistance or number of cycles. On the other hand, design configurations at higher γ_m values ($\gamma_m = 1.4, 1.5$) have lower magnitudes of stress cycles. These designs are governed by the fatigue resistance model uncertainty (X_m). The variations in α_i^2 factors for the 5 MW case are illustrated in Fig. 12 and Fig. 13. Comparable results are found for the 10 MW case as illustrated in Fig. 14 and Fig. 15.

The results above are based on a resistance model uncertainty X_m with COV $X_{mCOV} = 0.50$, which is estimated from available fatigue tests. A simple sensitivity study to investigate the importance of this COV is performed for the 5 MW case by assuming $X_{mCOV} = 0.25$. The results are summarized in Table 11 and Fig. 16. Note that the lower COV could probably be obtained in a narrow subset of the fatigue test data, covering only the application for this type of substructure.

7. Summary and conclusions

This paper demonstrates a probabilistic approach for reassessment of fatigue design rules for offshore wind turbine concrete structures. Offshore wind turbine loads accounting for the statistical distribution of turbulence intensity are estimated based on a fully-integrated model. Using available concrete fatigue tests, a fatigue reliability model is formulated based on the DNV code [17]. Reliability-based calibration of the material partial safety factor (γ_m) is demonstrated, while accounting for the relevant sources of uncertainties in both load and resistance models.

Safety margins in fatigue design of offshore concrete structures can be incorporated in terms on FDF and γ_m. The study showed that fatigue reliability is more sensitive to changes in γ_m. Two numerical examples of a concrete GBF supporting a 5 MW and 10 MW OWTs also showed that a lower γ_m can be used without compromising fatigue safety. Reducing the recommended value from $\gamma_m = 1.5$ to $\gamma_m = 1.1$ to 1.2 can lead to significant reduction in the required structural dimensions for both 5 MW and 10 MW cases. Lastly, the relative importance of stochastic input parameters are investigated. Depending on the assumed γ_m, reliability indices can be very sensitive to uncertainties related to concrete compressive strength (X_{fc}) and resistance model uncertainty (X_m).

A major limitation of the study is the lack of experimental concrete fatigue test data at lower stress amplitude cycles (high cycle fatigue tests). It is currently assumed that the same amount of uncertainty exists with concrete exposed to moderate stress levels. In addition, the study is limited to compression-compression fatigue cycles as assured by the prestressing, and does not take into account the effect of inspection which are difficult to perform and model in a probabilistic framework. Nonetheless, the presented framework can be applied to investigate fatigue reliability of other foundation concepts. Based on the main results presented, this study opens opportunities for life extension or repowering of offshore wind turbine concrete foundations approaching the end of their service lives.

CRediT authorship contribution statement

Joey Velarde: Conceptualization, Investigation, Methodology, Visualization, Writing - original draft. **Amol Mankar:** Conceptualization, Investigation, Methodology, Writing - review & editing. **Claus Kramhøft:** Conceptualization, Supervision. **John Dalsgaard Sørensen:** Methodology, Supervision, Validation.

Declaration of Competing Interest

The authors declare that they have no known competing financial interests or personal relationships that could have appeared to influence the work reported in this paper.

Acknowledgements

This research work was performed within the European project INFRASTAR, which has received funding from the European Union's Horizon 2020 research and innovation programme under the Marie Skłodowska-Curie grant agreement No 676139.

References

[1] Esteban MD, et al. Gravity based support structures for offshore wind turbine generators: Review of the installation process, eng. Ocean Eng 2015;110:281–91. https://doi.org/10.1016/j.oceaneng.2015.10.033. ISSN: 18735258, 00298018.
[2] Dolores Esteban M, Lopez-Gutierrez Jose-Santos, Negro Vicente. Gravity-based foundations in the offshore wind sector. J Marine Sci Eng 2019;7(3):64.
[3] Ronold Knut O, Wedel-Heinen Jakob, Christensen Carl J. Reliability-based fatigue design of wind-turbine rotor blades. Eng Struct 1999;21(12):1101–14.
[4] Veldkamp Dick. A probabilistic evaluation of wind turbine fatigue design rules.

Wind Energy 2008;11(6):655–72.
[5] Sørensen John D, Toft Henrik S. Probabilistic design of wind turbines. Energies 2010;3(2):241–57.
[6] Toft Henrik Stensgaard, Sørensen John Dalsgaard. Reliability-based design of wind turbine blades. Struct Saf 2011;33(6):333–42.
[7] Toft Henrik Stensgaard, et al. Uncertainty modelling and code calibration for composite materials. J Compos Mater 2013;47(14):1729–47.
[8] Nejad Amir Rasekhi, Gao Zhen, Moan Torgeir. On long-term fatigue damage and reliability analysis of gears under wind loads in offshore wind turbine drivetrains. Int J Fatigue 2014;61:116–28.
[9] Sørensen John Dalsgaard. Reliability-Based Calibration of Fatigue Safety Factors For Offshore Wind Turbines. Int J Offshore Polar Eng 2012;22:03.
[10] Marquez-Dominguez Sergio, Sørensen John D. Fatigue reliability and calibration of fatigue design factors for offshore wind turbines. Energies 2012;5(6):1816–34.
[11] Dong Wenbin, Moan Torgeir, Gao Zhen. Fatigue reliability analysis of the jacket support structure for offshore wind turbine considering the effect of corrosion and inspection. Reliab Eng Syst Saf 2012;106:11–27.
[12] Mai Quang A, et al. Prediction of remaining fatigue life of welded joints in wind turbine support structures considering strain measurement and a joint distribution of oceanographic data. Marine Struct 2019;66:307–22. https://doi.org/10.1016/j.marstruc.2019.05.002. URL. ISSN: 0951-8339, URL: http://www.sciencedirect.com/science/article/pii/S095183391830217X.
[13] Horn Jan-Tore, Leira Bernt J. Fatigue reliability assessment of offshore wind turbines with stochastic availability. Reliab Eng Syst Saf 2019:106550.
[14] Madsen Henrik O, Krenk Steen, Lind Niels Christian. Methods of structural safety. Courier Corporation; 2006.
[15] JCSS JCSS. Probabilistic model code. In: Joint Committee on Structural Safety; 2001.
[16] Faber MH, Sørensen John Dalsgaard. Reliability-based code calibration: the JCSS approach. In: 9th International Conference on Applications of Statistics and Probability in Civil Engineering. Millpress. 2003, p. 927–35.
[17] Det Norsk Veritas. Offshore Concrete Structures-DNV OS-C502. In: Det Norsk Veritas, Norway; 2012.
[18] fib. FIB Model Code for concrete structures 2010; 2010.
[19] Eurocode No. 2, Design of concrete structures. In: European Committee for Standardization; 1992.
[20] International Standards Organization. ISO 2394: 2015: General principles on reliability for structures; 2015.
[21] International Electrotechnical Commission et al. IEC 61400-1. In: Wind Turbines—Part 1: Design Requirements; 2019.
[22] International Electrotechnical Commission et al. IEC 61400-3. In: Wind Turbines—Part 3: Design Requirements for Offshore Wind Turbines; 2009.
[23] GL DNV. Support structures for wind turbines. In: Standard DNVGL-ST-0126; 2018.
[24] GL DNV. Fatigue design of offshore steel structures. In: Recommended Practice DNVGL-RP-C203 20; 2016.
[25] Mankar Amol et al. Probabilistic reliability framework for assessment of concrete fatigue of existing RC bridge deck slabs using data from monitoring. Eng Struct. 2019;201:109788. ISSN: 0141-0296. doi: 10.1016/j.engstruct.2019.109788. URL: http://www.sciencedirect.com/science/article/pii/S0141029619300045.
[26] Velarde Joey, et al. Uncertainty modeling and fatigue reliability assessment of offshore wind turbine concrete structures. Int J Offshore Polar Eng 2019;29(02):165–71.
[27] Sørensen JD, Toft HS. Safety Factors–IEC 61400-; 4—Background Document. In: DTU Wind Energy-E-Report-0066 (EN); 2014.
[28] Thomsen Jørn H, Forsberg Torben, Bittner Robert. Offshore wind turbine foundation: the COWI experience. In: International Conference on Offshore Mechanics and Arctic Engineering. vol. 42711; 2007, p. 533–40.
[29] Peire Kenneth, Nonneman Hendrik, Bosschem Eric. Gravity base foundations for the thornton bank offshore wind farm. Terra et Aqua 2009;115(115):19–29.
[30] Velarde Joey, et al. Fatigue reliability of large monopiles for offshore wind turbines. Int J Fatigue 2020;134:105487.
[31] Velarde Joey, Kramh0ft Claus, Sørensen John Dalsgaard. Global sensitivity analysis of offshore wind turbine foundation fatigue loads. Renewable Energy. 2019. ISSN: 0960-1481. doi: 10.1016/j.renene.2019.03.055. URL: http://www.sciencedirect.com/science/article/pii/S096014811930360X.
[32] Larsen Torben Juul, Hansen Anders Melchior. How 2 HAWC2, the user's manual. In: Target vol. 2; 2015, p. 2.
[33] Jonkman Jason et al. Definition of a 5-MW reference wind turbine for offshore system development. Tech. rep. National Renewable Energy Laboratory (NREL), Golden, CO., 2009.
[34] Bak Christian et al. Description of the DTU 10 MW reference wind turbine. In: DTU Wind Energy Report-I-0092 5, 2013.
[35] Mann Jakob. Wind field simulation. Probabilistic Eng Mech 1998;13(4):269–82.
[36] Glauert Hermann. Airplane propellers. Aerodynamic theory. Springer; 1935. p. 169–360.
[37] Hansen Martin OL, Madsen Helge Aagaard. Review paper on wind turbine aerodynamics. J Fluids Eng 2011;133(11):114001.
[38] Morison JR, Johnson JW, Schaaf SA, et al. The force exerted by surface waves on piles. J Petrol Technol 1950;2(05):149–54.
[39] Palmgren Arvid. Die lebensdauer von kugellagern. Z Ver Dtsch Ing 1924;68(14):339–41.
[40] Miner Milton A, et al. Cumulative damage in fatigue. J Appl Mech 1945;12(3):159–64.
[41] Sørensen Eigil V. Fatigue life of high performance grout in dry and wet environment for wind turbine grouted connections. Nordic Concr Res 2011;44:1–10.
[42] Lohaus Ludger, Oneschkow Nadja, Wefer Maik. Design model for the fatigue behaviour of normal-strength, high-strength and ultra-high-strength concrete. Struct Concr 2012;13(3):182–92.
[43] Lantsoght EOL. Fatigue of concrete under compression: Database and proposal for high strength concrete. In: Report nr. 25.5-14-04, 2014.
[44] Thiele Marc. Experimentelle Untersuchung und Analyse der Schadigungsevolution in Beton unter hochzyklis-chen Ermudungsbeanspruchungen. 2016.
[45] Folsø Rasmus, Otto Sven, Parmentier Guy. Reliability-based calibration of fatigue design guidelines for ship structures. Marine Struct 2002;15(6):627–51.
[46] Toft Henrik Stensgaard, et al. Uncertainty in wind climate parameters and their influence on wind turbine fatigue loads. Renew Energy 2016;90:352–61.